CHEMISTRY
A EUROPEAN JOURNAL

FULL PAPER

DOI: 10.1002/chem.201301903

Tuning Redox Chemistry and Photophysics in Core-Substituted Tetraazaperopyrenes (TAPPs)

Sonja Geib,[a] Susanne C. Martens,[a] Michaela Märken,[a] Arina Rybina,[b] Hubert Wadepohl,[a] and Lutz H. Gade*[a]

Abstract: Core substitution of tetraazaperopyrenes (TAPPs) has been achieved, and with it, considerable variation of their photo- and redox-chemical properties. Through Suzuki cross coupling starting from the fourfold core-brominated tetraazaperopyrene, aryl-substituted TAPPs were synthesized, which displayed very high fluorescence quantum yields (up to 100%) in solution. Besides the Suzuki reactions, Stille and Sonogashira cross-couplings were also found to be suitable methods for core derivatization, as demonstrated in the syntheses of alkynyl-substituted tetraazaperopyrene congeners. Furthermore, TAPPs incorporating intramolecular donor–acceptor combinations of aromatic units (**8**, **9**) were accessible by coupling the electron-poor peropyrene core with electron-rich aromatic units, which act as strong electron donors. Finally, C-heteroatom coupling (O, S, N) gave rise to novel TAPP derivatives with strongly modified redox-chemical behaviour and photophysics in the solid state as well in solution. In particular, TAPP derivatives displaying red fluorescence were obtained for the first time.

Keywords: electrochemistry · electron transfer · fluorescence · photophysics · redox chemistry

Introduction

The widespread interest in perylene-3,4,9,10-tetracarboxydiimides (PDIs) during the past fifteen years[1] has been due to their manifold applications as functional fluorescence dyes and organic semiconductors in thin-film transistors or light-emitting diodes.[2,3] Efficient synthetic methods for the selective functionalization of the polycyclic aromatic core were at the heart of this dynamic development.[4] Appropriate substitution, introducing electron-releasing or -withdrawing groups, allowed the tuning not only of the frontier orbital energies, but also the photophysics of the PDI derivatives. In fact, the latter was equally modified by substituent-induced distortion from planarity of the polycyclic aromatic core.[5] These considerable research efforts have rendered PDIs the most intensely studied class of organic dyes.

In recent years, we developed an efficient synthesis for 1,3,8,10-tetraazaperopyrenes (TAPPs),[6,7] a class of polyheterocyclic aromatics possessing photo- and redox-chemical properties related to PDIs. Similarly to the latter, TAPPs are electron acceptors in which the two carboximido units at the perylene core are replaced by two fused pyrimidine rings. Their synthesis from 4,9-diaminoperylene-quinone-3,10-diimine[8] only allowed limited functionalization at the 2- and 9-positions.[9] Because these lie along the principal molecular axis, and thus, are in the nodal plane of the frontier orbitals of the molecules, their effect on the photo- and redox-chemical properties was negligible.

However, we recently reported the synthesis of fourfold core-chlorinated and -brominated TAPP derivatives, and demonstrated that these materials possess n-channel semiconducting properties suitable for the fabrication of air-stable organic thin-film transistors with good electron mobilities.[10] From a synthetic point of view, the chlorinated and brominated TAPPs should be ideal starting compounds for further derivatisation of the peropyrene core, and thus, for a systematic development of this class of functional organic dyes.

Herein, we describe for the first time the syntheses of core-substituted tetraazaperopyrene compounds and the ways in which different types of substituents affect their properties. The readily accessible fluoroalkylated 2,9-bis-heptafluoropropyl-4,7,11,14-tetrabromo-1,3,8,10-tetraazaperopyrene[10b] proved to be a versatile starting material that could be derivatized through nucleophilic substitution or Pd-catalyzed C–C or C–N coupling reactions.

Results and Discussion

Synthesis, structural characterization, and photophysics of aryl- and alkynyl-substituted TAPPs: In a first effort to modify the TAPP core, a Suzuki cross-coupling reaction of the fourfold core-chlorinated TAPP **I** (Scheme 1)[10a] with

[a] Dr. S. Geib, Dr. S. C. Martens, M. Märken, Prof. H. Wadepohl, Prof. L. H. Gade
Anorganisch-Chemisches Institut, Universität Heidelberg
Im Neuenheimer Feld 270, 69120 Heidelberg (Germany)
Fax: (+49) 6221-545609
E-mail: lutz.gade@uni-hd.de

[b] A. Rybina
Cellnetworks Cluster and Institute for Physical Chemistry
Universität Heidelberg, Im Neuenheimer Feld 267/BQ0007
69120 Heidelberg (Germany)

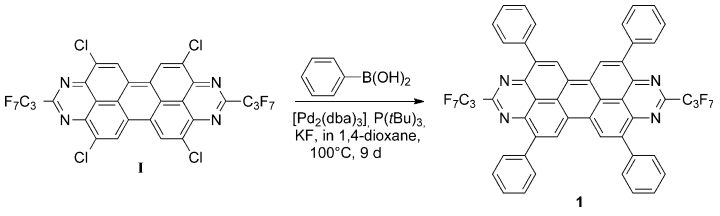

Scheme 1. Suzuki cross-coupling reaction of a chlorinated TAPP **I**.

phenylboronic acid, using $[Pd_2(dba)_3]/P(tBu)_3$ as the catalyst system, was performed.[11] The desired product (**1**) could be isolated and fully characterized after extended reaction times (9 days at 100 °C), but less than fourfold-substituted TAPP moieties and dehalogenated starting material were also detected in the reaction mixture, which accounted for the moderate yield (42 %).

As bromides are commonly known to be more reactive than chlorides in cross-coupling or substitution reactions,[12] all further synthetic transformations were performed starting from 2,9-bis-heptafluoropropyl-4,7,11,14-tetrabromo-1,3,8,10-tetraazaperopyrene **II** (Scheme 2).[10b] This derivative was chosen from the known series of core-brominated TAPPs because of its solubility in organic solvents (due to the C_3-perfluorinated alkyl chain) and its availability in sufficient quantities. Moreover, as we have reported previously, all tetraazaperopyrene compounds are characterised by the nodal plane of their molecular frontier orbitals along the principal molecular axis connecting carbon atoms 2 and 9.[6,9] Consequently, the length of the perfluorinated alkyl chain does not significantly influence their photophysical and electrochemical properties. Through the reaction of **II** with *para*-substituted phenylboronic acids in the presence of a Pd catalyst and a base, the fourfold aryl-substituted tetraazaperopyrenes **2**, **3**, and **4** were isolated as bright orange solids. The yields were the highest for the *para*-carboxyethyl derivative, and decreased with the electron-withdrawing character of the *para*-substituent at the phenyl ring. Overall, higher yields were obtained with $[Pd(dppf)Cl_2]$ as a pre-catalyst[13] than with the $[Pd_2(dba)_3]/P(tBu)_3$ system. For all transformations, no dehalogenation of the starting compound was detected, and only the completely substituted derivatives were isolated from the reaction mixtures, in contrast to the reactions of its chlorinated analogue.

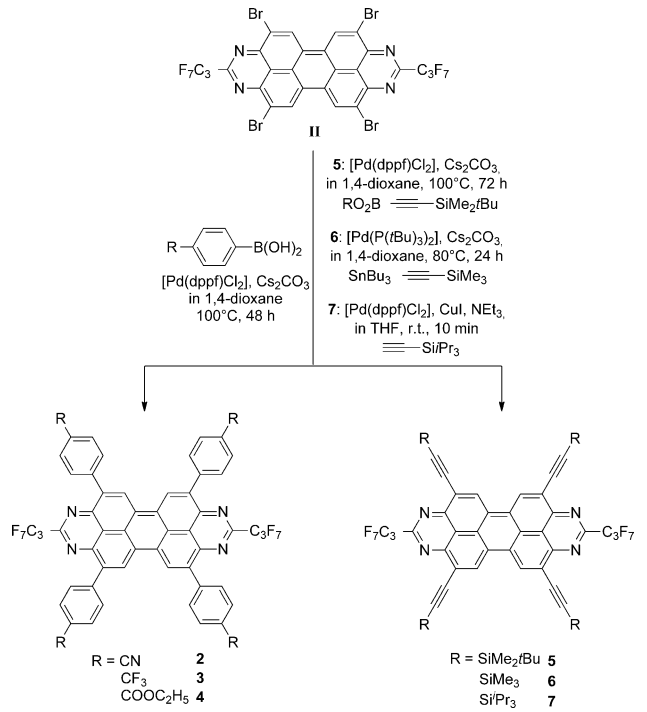

Scheme 2. Synthesis of the phenyl- and alkynyl-substituted tetraazaperopyrenes **2**–**7** starting from the brominated TAPP congener **II**.

As a next step and as a new structural motif, the introduction of alkynyl substituents was investigated. The synthesis of fourfold alkynyl-silyl-substituted TAPP derivatives was accomplished via Suzuki (**7**), Stille (**8**), and Sonogashira (**9**) cross-coupling reactions with the corresponding boronic ester, organotin compound, or terminal alkyne (Scheme 2). Among these transformations, the Sonogashira reaction gave the highest yield of the desired product and could be performed under the mildest conditions. In this case, a tetraalkynylation of the peropyrene core was achieved at room temperature after very short reaction times.

We note that the solubility of the tetraazaperopyrene compounds is enhanced remarkably by the introduction of aryl or alkynyl substituents. The derivatives **5** and **7** are even completely soluble in nonpolar solvents such as pentane or hexane, which can be attributed to the solubilizing effect of the SiR_3 groups.

Monoclinic crystals of compound **6** suitable for X-ray diffraction were grown from THF solution. The molecules have crystallographic inversion symmetry (Figure 1). In analogy to the previously reported 2,9-(C_3F_7)-TAPP derivatives,[10] the heptafluoropropylalkynyl chains point in opposite directions above and below the tetraazaperopyrene core.

The alkynyl substituents barely influence the structure of the peropyrene core, the small C3–C4–C10–C9′ torsion angle of about 3° being within the range observed for unsubstituted TAPPs. The arrangement of the molecules of **6** in the solid state is, however, different from the known structural arrangements of core-brominated or core-chlorinated TAPP congeners (Figure 2).[10] In both cases, slip-stacked face-to-face arrangements of the molecules are adopted. However, whereas there is only one kind of stack for the core-halogenated TAPP derivatives, the molecules of compound **6** form two independent stacks along the shortest cell axis *a*, which are rotated by about 80° relative to each other. The interplanar distance between two neighbouring molecules in one stack is 3.41 Å, which is very similar to the π–π-distance of the brominated starting compound **3** (3.39 Å). The bulky alkynyl substituents at the peropyrene core do not seem to inhibit close contact between the aromatic cores, but induce the twisted arrangement of the stacks with respect to each other.

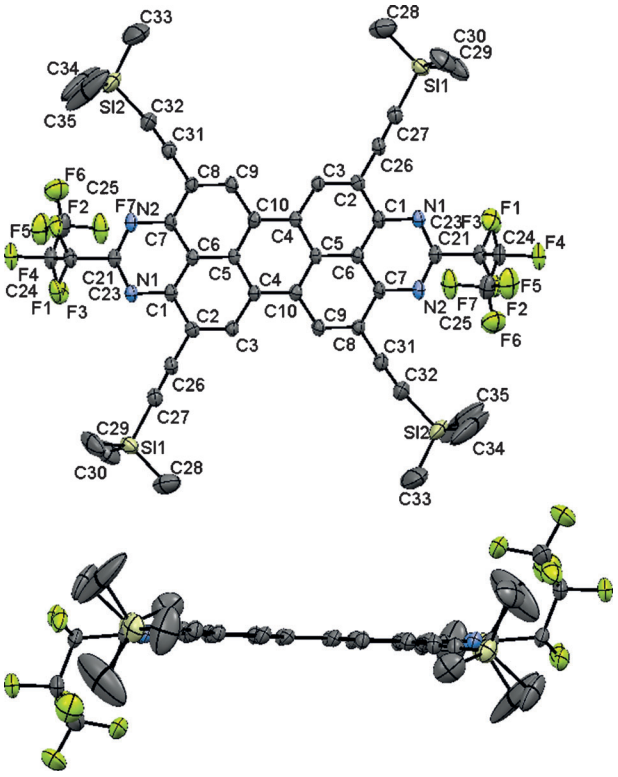

Figure 1. Molecular structure of **6**: top view (top) and side view (bottom). Thermal ellipsoids are drawn at the 50% probability level. Hydrogen atoms are omitted for clarity. Principal bond lengths [Å]: Si1/Si2–C27/C32 1.837(5)/1.837(5), N1/N2–C21 1.336(6)/1.334(6), N1/N2–C1/C7 1.346(5)/1.338(5), C1/C7–C6 1.414(6)/1.411(6), C1/C7–C2/C8 1.443(6)/1.451(6), C2/C8–C3/C9 1.373(6)/1.365(6), C2/C8–C26/C31 1.429(6)/1.433(6), C3/C9–C4/C10′ 1.425(6)/1.434(6), C4–C10 1.413(6), C4/C10′–C5 1.427(6)/1.420(6), C26/C31–C27/C32 1.204(7)/1.206(7).

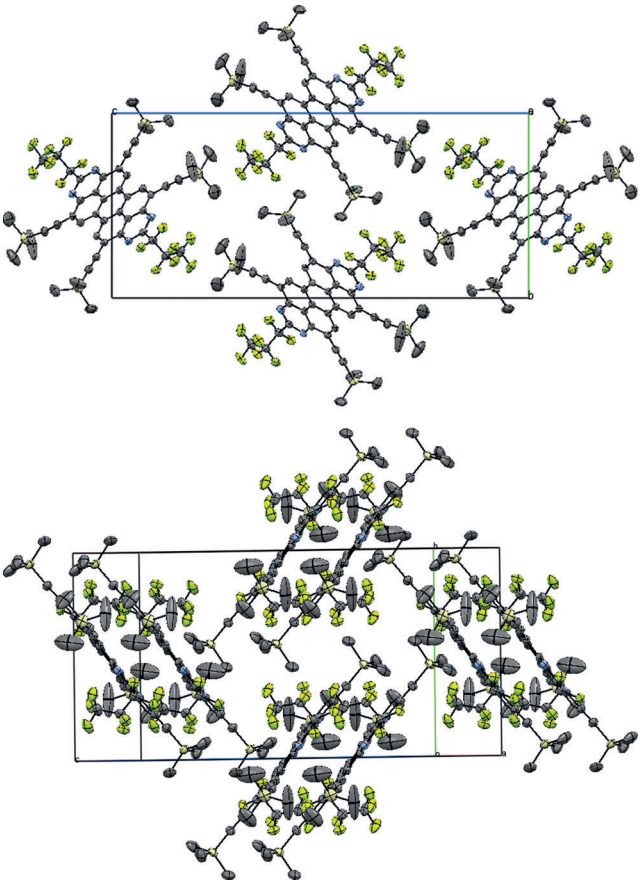

Figure 2. Packing pattern of **6** in the solid state: top: view along *b*; bottom: view perpendicular to the stacks.

For the investigation of the influence of the newly introduced core substituents, the optical properties of **1**–**7** were examined through UV/Vis and fluorescence spectroscopy. The tetraazaperopyrenes show no significant solvatochromism in organic solvents; however, the polarity of the solvents does influence the fluorescence quantum yields, as expected. The absorption spectrum of the core-brominated starting compound **II** displays a strong absorption band from 400 to 500 nm with a maximum at 475 nm. The band displays a pronounced vibrational progression ($\Delta\nu \approx 1400\ cm^{-1}$) that can typically be seen for the $\pi^*\leftarrow\pi$ transition in perylene derivatives.[14,15] The fourfold phenyl-substituted TAPP derivatives **1**–**4** are bright orange solids and yellow in solution, with a strong green fluorescence in dilute solutions. Their UV/Vis spectra, displayed in Figure 3, are characterised by an intense absorption band with a maximum that is bathochromically shifted with respect to the parent compound **II** by 15 nm to about 490 nm, and thus, is slightly broader than in the corresponding spectrum of **II**, which might be attributed to the conformational flexibility of the four phenyl rings attached to the peropyrene core. The alkynyl-substituted TAPPs **5**–**7** exhibit an absorption band with a maximum at 515 nm (Figure 3, top). This bathochromic shift compared to **1**–**4** may be explained by the conjugation of the alkynyl substituents with the peropyrene core and the resulting smaller HOMO–LUMO gap. In contrast to the phenyl-substituted TAPPs, the absorption spectra of **5**–**7** are characterised by sharp bands with a well-resolved vibronic fine structure when recorded in nonpolar solvents. In addition to the $S_1\leftarrow S_0$ transition characteristic of TAPP derivatives, the $S_2\leftarrow S_0$ transition can also be observed clearly (Figure 3, bottom). The superior spectral resolution may be attributed to the rigid molecular structure of the alkynyl-substituted derivatives **5**, **6**, and **7**.

The emission bands of the core-substituted TAPPs are mirror images of the corresponding absorption bands (Figure 4), indicating that the molecular geometries of the electronic ground state and excited state are similar.[14] The brominated TAPP **II** exhibits only weak fluorescence in THF (max: 486 nm), which can be attributed to the quenching effect of the heavy bromine atoms. The emission maxima of the phenyl-substituted TAPPs **1**–**4** were detected at about 520 nm. The overall highest fluorescence quantum yields Φ of up to unity (100%) were found for these compounds. The bulky phenyl rings that are twisted out of the tetraazaperopyrene plane inhibit intermolecular aggregation perfectly. Though not a general rule, the emission quantum yields of planar molecules may increase when phenyl groups

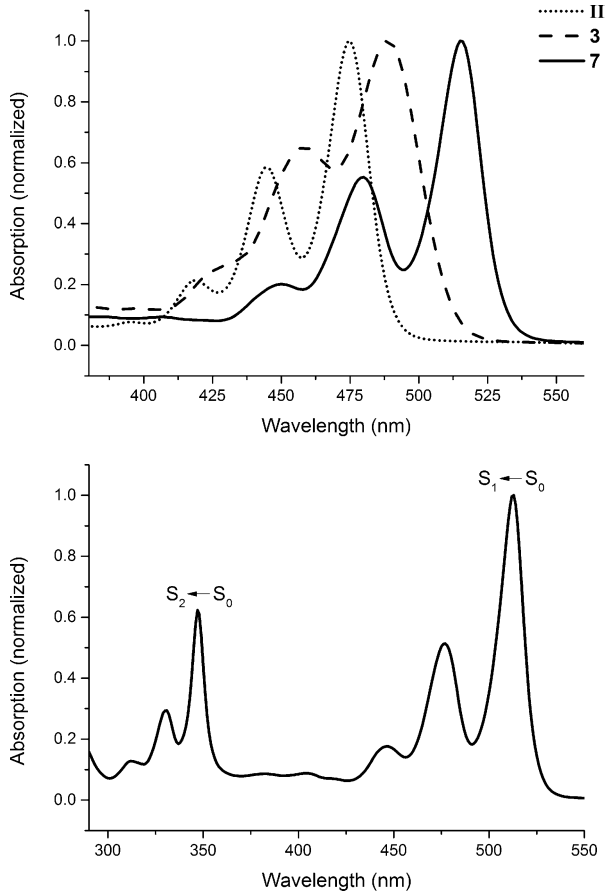

Figure 3. Detail of the normalized UV/Vis absorption spectra of **II**, **3**, and **7** in THF showing the band that is attributed to the first $\pi^*\leftarrow\pi$ transition centred on the perylene core with the typical vibronic fine structure (top). UV/Vis spectrum of **7** in pentane showing the transitions to the first and second excited $\pi^*\leftarrow\pi$ states (bottom).

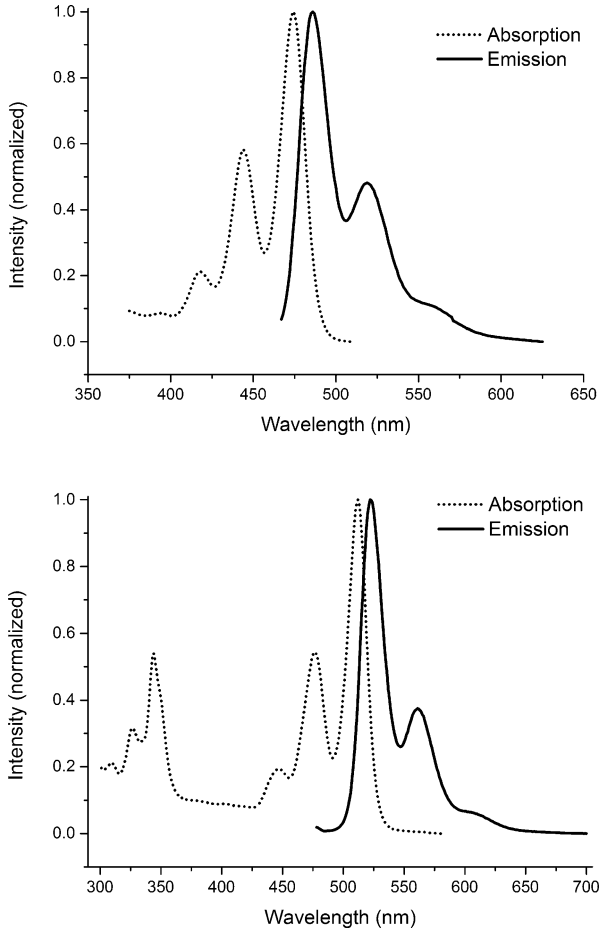

Figure 4. Absorption and mirror-image emission spectrum of **II** (top) and **7** (bottom) recorded in THF.

are attached to such planar systems, as noted previously.[16] The absorption and emission data of the tetraazaperopyrene derivatives **II**, **1**–**4**, and **5**–**7** are summarized in Table 1.

On the other hand, the alkynyl-substituted tetraazaperopyrenes **5**–**7**, which possess a more rigid molecular structure, only exhibit fluorescence quantum yields in the range 35–45% in THF. Aggregation can be ruled out as a reason for these lower quantum yields, as a dilution series affected neither the band structure nor the observed quantum yields. A possible mechanism for a partial quenching of the fluorescence might therefore be the stronger molecule–solvent interactions of compounds **5**–**7**, in which the TAPP core is not shielded effectively by the alkynyl substituents against solvent contacts. In nonpolar solvents such as pentane, however, the fluorescence quantum yields rise to about 60% but still do not reach unity, which indicates that other mechanisms of nonradiative deactivation are likely to operate. The Stokes shifts of the corresponding emission (at ≈525 nm) are thus much smaller for the alkynyl-substituted TAPPs (10 nm) than for the phenyl-substituted TAPPs (30 nm), indicating that the molecular geometries in the ground state and excited state are very similar for these rigid molecules.

Table 1. Absorption and emission data of **II**, **1**–**4**, and **5**–**7**.

	λ_{max} [nm] (log ε)	$\Delta\nu$ [cm^{-1}]	λ_{em} [nm] (Stokes shift)	Φ	τ [ns]
II	475 (4.91)	1419	486 (11)	0.12	2.1
1	500 (4.76)	1322	527 (27)	0.85	3.2
2	492 (4.75)	1320	518 (24)	1.00	2.8
3	489 (4.80)	1384	512 (23)	0.96	2.8
4	497 (4.83)	1293	523 (26)	0.79	2.8
5	513 (4.96)	1427	523 (10)	0.35	2.1
6	512 (5.04)	1433	522 (10)	0.45	2.1
7	516 (5.02)	1453	525 (9)	0.37	2.0

The fluorescence lifetimes for **II** and **1**–**7** show exclusively monoexponential behaviour and lie in the range of about 2–3 ns (Table 1).

Electrochemistry and theoretical modelling of the frontier orbital energies of TAPP derivatives 1–7: The electrochemical properties of the new core-functionalized TAPP derivatives were investigated by cyclic voltammetry. The cyclic voltammograms of the phenyl-substituted tetraazaperopyrenes **1**–**4** as well as the alkynyl-substituted compounds **5**–**7** are characterised, as expected, by two reversible redox waves that can be attributed to the subsequent formation of

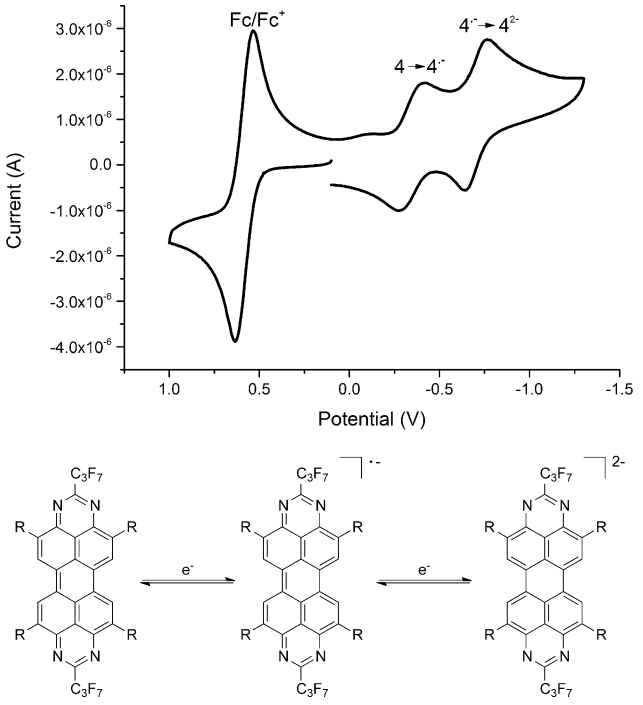

Figure 5. Cyclic voltammogram of compound **4** in THF (top) and general representation of the reversible reduction to the radical anionic and dianionic TAPP species (bottom).

the corresponding radical anion and the dianionic species, respectively (Figure 5).[6] In comparison to the brominated starting material **II**, the first reduction half wave for **1**–**7** is shifted to more negative potentials.[10b]

The redox-chemical data derived from the cyclic voltammograms allowed the determination of the corresponding LUMO energies using the redox potential of ferrocene as a point of reference (Table 2).[17] In addition, the ground-state geometries of all the TAPP derivatives were modelled by DFT using the B3PW91 functional and the 6–31 g(d,p) basis set; the computed HOMO and LUMO energies are also summarised in Table 2. We note that for the phenyl- (**1**–**4**) and alkynyl-substituted (**5**, **6**, **7**) TAPPs, the calculated and measured LUMO energy levels are in fairly good agreement.

Table 2. Summary of the reduction potentials (measured relative to Fc/Fc$^+$ and referenced to SCE), LUMO energies derived thereof, and computed HOMO and LUMO energies.

	E_{Red1} [V][a]	E_{Red2} [V][a]	$E_{LUMO(CV)}$ [eV][b]	$E_{LUMO(DFT)}$ [eV][c]	$E_{HOMO(DFT)}$ [eV][c]
II	−0.18	−0.56	−4.04	−4.10	−6.71
1	−0.47	−0.84	−3.76	−3.51	−5.98
2	−0.26	−0.65	−3.96	−4.29	−6.77
3	−0.29	−0.69	−3.92	−4.00	−6.52
4	−0.35	−0.70	−3.87	−3.78	−6.26
5	−0.25	−0.63	−3.97	−3.77	−6.07
6	−0.22	−0.60	−3.99	−3.74	−6.05
7	−0.26	−0.60	−3.95	−3.77	−6.05

[a] **II**, **1**–**7**: measured relative to Fc/Fc$^+$ and referenced to SCE. [b] Determined according to literature methods using Fc/Fc$^+$ as internal standard (E_{HOMO}(Fc) = −4.8 eV). [c] Calculated at the B3PW91/6–31 g(d,p) level of theory.

Synthesis and properties of donor–acceptor TAPPs: Given the successful synthesis of aryl- and alkynyl-substituted tetraazaperopyrene compounds (**1**–**7**) and the established property of the TAPP core as an electron acceptor, we combined the latter with electron donor units in the four core substituent positions. This would allow the investigation of intramolecular charge-transfer phenomena, and thus, the suitability of the TAPPs to act as functional (redox) units in more complex organic dyes. Suzuki reactions of **II** with the sterically demanding, electron-rich boronic acids, pyrene-1-boronic acid and 4-(diphenylamino)phenylboronic acid, yielded the desired donor–acceptor TAPP derivatives **8** and **9**, respectively (Scheme 3), both of which were isolated as dark green solids.

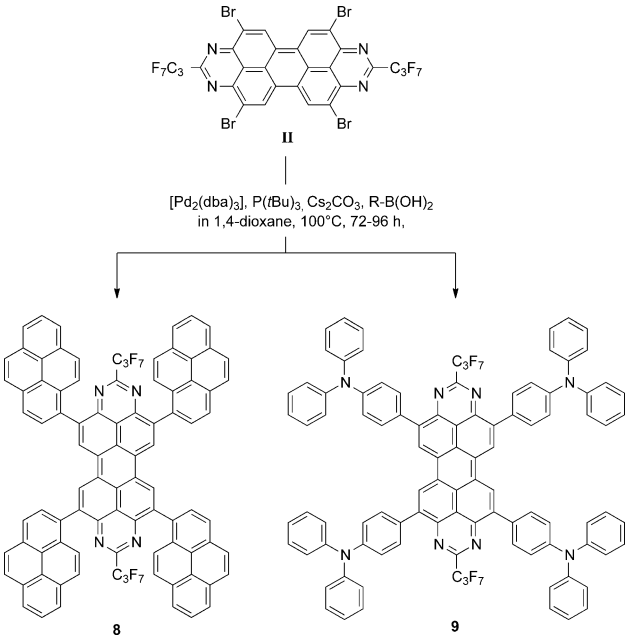

Scheme 3. Suzuki coupling reaction of sterically demanding, electron-rich boronic acids with TAPP **II**.

The photophysical properties of **8** and **9** were studied in THF and toluene and found to be remarkably different from those of the aryl- and alkynyl-substituted TAPPs discussed above. Even though both solids are dark green in the solid state, solutions of compound **8** were found to be deep red, whereas **9** gave blue solutions.

The absorption spectra of both compounds display three major groups of bands (Figure 6 and Table 3). First, the typical absorption assigned to the π*←π transition of the TAPP core was observed at about 450, and thus, is hypsochromically shifted by about 25 nm with respect to the parent compound **II**. However, the vibronic fine structure is much less pronounced compared to the TAPP derivatives discussed above, especially for compound **9**. This observation might

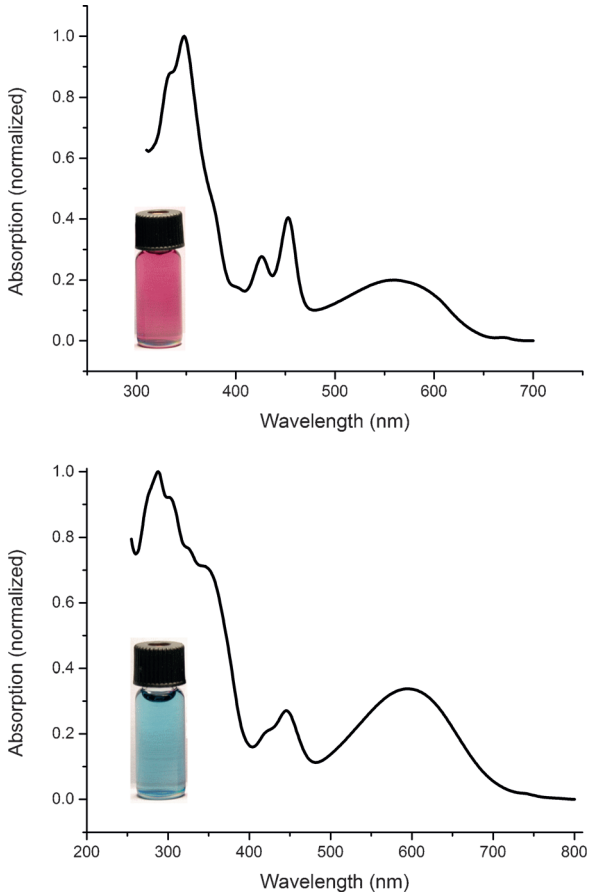

Figure 6. Normalized absorption spectra of TAPP **8** in toluene (top) and TAPP **9** in THF (bottom) and their corresponding colours in highly dilute solutions.

Table 3. Summary of the absorption properties found for the TAPP derivatives **8** and **9** in THF and toluene.

	Substituent		Peropyrene core			CT band	
	λ_{max} [nm]	log ε	λ_{max} [nm]	log ε	$\Delta\nu$ [cm^{-1}]	λ_{max} [nm]	log ε
8 (THF)	346	5.05	447	4.47	1325	524	3.95
8 (toluene)	348	5.28	453	4.88	1399	560	4.58
9 (THF)	288	5.05	446	4.49	–	594	4.58
9 (toluene)	347	4.95	451	4.53	1356	611	4.64

be attributed to considerable conjugation between the peropyrene core and the four electron-rich substituents.[18,19] Second, an intense band at shorter wavelengths (<380 nm) originates from excitations located on the four pyrene and 4-(diphenylamino)phenyl substituents themselves. A third, broad, structureless band is observed in the region between 500 and 700 nm. The latter closely resembles the charge-transfer absorption bands observed for perylenetetracarboxydiimide (PDI) derivatives that have electron-donating substituents at the aromatic core.[18,19] It is thus assumed to originate from a photo-induced charge transfer from the electron-rich substituents to the electron-deficient peropyrene core. This is consistent with the observed marked solvent dependence of this band compared to the π*←π transitions centred on the TAPP core or the substituents. Unfortunately, limitations imposed by the solubility of **8** and **9** precluded a wider systematic variation of solvent polarity.

The cyclic voltammograms of the donor–acceptor systems **8** and **9** were also found to be remarkably different from those of compounds **1**–**7**, mirroring the different UV/Vis absorption spectra. For both compounds, the reversible uptake of two electrons is observed at significantly more negative potentials owing to the strongly electron-donating nature of the substituents at the peropyrene core.

Apart from these typical reduction waves at negative potentials, oxidation of the polycyclic aromatics also takes place within the scanned potential window. For the pyrenyl-substituted TAPP **8**, only irreversible redox waves were detected at positive potentials (Figure 7, top), but for the four-fold 4-(diphenylamino)phenyl-substituted TAPP **9**, one narrow, quasi-reversible oxidation wave was observed, which corresponds to the formation of four radical cations located on the four $C_6H_4NPh_2$ substituents (Figure 7, bottom).

The calculated LUMO (and HOMO) energies of the donor–acceptor TAPPs (**8**, **9**), based on DFT modelling as

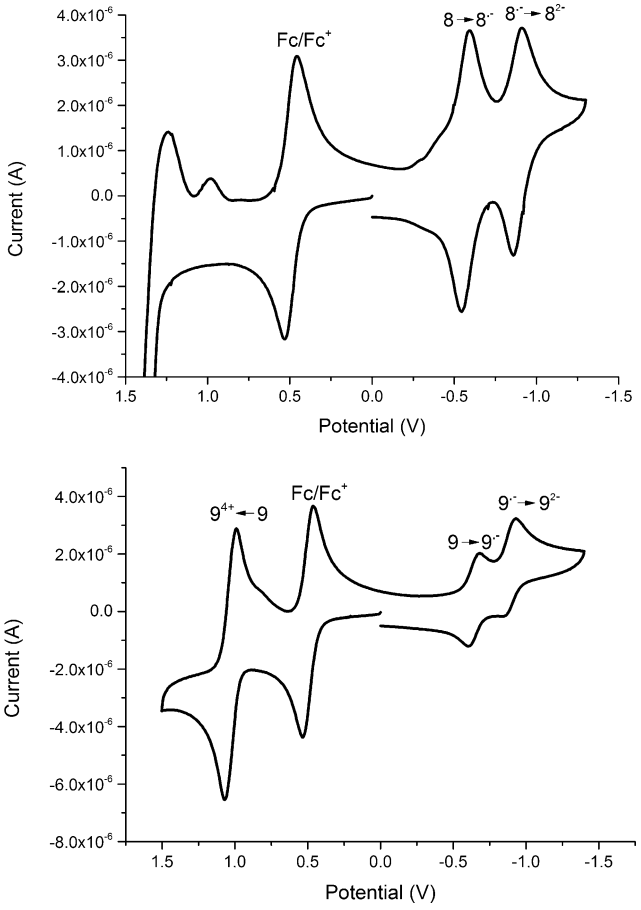

Figure 7. Cyclic voltammograms of **8** (top) and **9** (bottom) recorded in CH_2Cl_2 (sweep rate 50 mV s^{-1}, supporting electrolyte nBu$_4$NPF$_6$, reference SCE).

Table 4. Summary of the reduction (and oxidation) potentials, the LUMO (and HOMO) energies derived from these data, and the computed HOMO and LUMO energies.

	E_{Red1} [V][a]	E_{Red2} [V][a]	$E_{LUMO(CV)}$ [eV][b]	$E_{LUMO(DFT)}$ [eV][c]	E_{Ox} [V][a]	$E_{HOMO(CV)}$ [eV][b]	$E_{HOMO(DFT)}$ [eV][c]
II	−0.18	−0.56	−4.04	−4.10			−6.71
8	−0.57	−0.89	−3.64	−3.49			−5.50
9	−0.64	−0.90	−3.66	−3.28	1.03	−5.33	−5.02

[a] **II**: measured relative to Fc/Fc^+ and referenced to SCE. **8**–**9**: Measured against SCF in CH_2Cl_2. [b] Determined according to literature methods using Fc/Fc^+ as internal standard ($E_{HOMO}(Fc) = -4.8$ eV). [c] Calculated at the B3PW91/6–31 g(d,p) level of theory.

described above for the other TAPP derivatives, differ somewhat from the values derived from the cyclic voltammograms (Table 4). However, it is generally apparent that, as expected, the electron-donating substituents influence the HOMO to a greater extent than the LUMO.

The frontier Kohn–Sham orbitals of compounds **8** and **9** support the interpretation that these tetraazaperopyrenes are intramolecular donor–acceptor molecules: the HOMO is localized mainly on the peripheral substituents attached to the TAPP core, whereas the LUMO is typically localized at the peropyrene core (Figure 8). A closer inspection of the structure of the HOMO reveals that there is significant conjugation between the peripheral substituents and the TAPP core. The observed charge-transfer band (vide supra) is therefore appropriately interpreted as a primarily photo-induced electron transfer from the electron-rich peripheral arene units (i.e., the HOMO) to the electron-deficient peropyrene core (i.e., the LUMO).

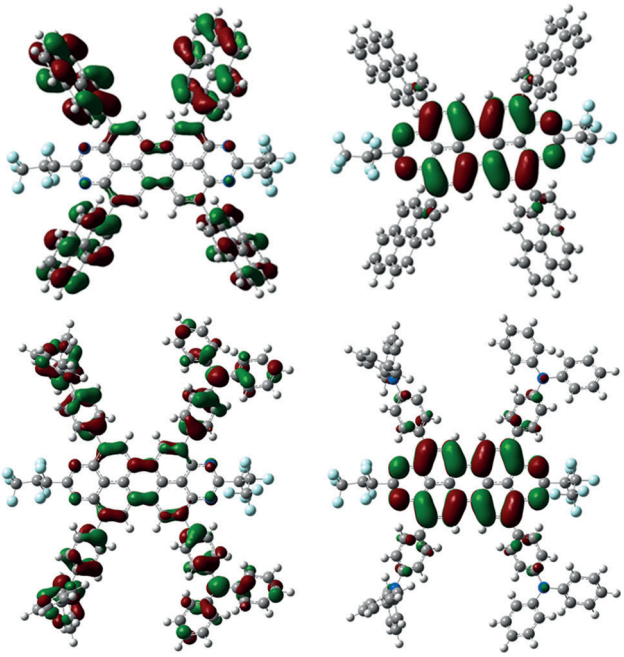

Figure 8. Visualized HOMO and LUMO of TAPP **8** (top) and TAPP **9** (bottom).

Synthesis and properties of heteroatom-substituted tetraazaperopyrenes: The photophysics and redox-chemical behaviour of the core-substituted TAPP derivatives were thought to be affected most significantly by the introduction of heteroatom substituents at the polycyclic aromatic core. This has already been manifested in the comparison of the halogenated TAPPs **I** and **II** with the unsubstituted parent compound. To this end, C–heteroatom (O, S, N) coupling reactions of **II** were investigated. The main objective was to influence the absorption and emission colours significantly. Reaction of **II** with phenol under basic conditions gave **10** as a red solid. For the reaction of **II** with thiophenol, phase-transfer catalysis was employed to yield **11** as a violet solid, and Pd-catalysed Buchwald–Hartwig amination with aqueous KOH base led to the four-fold nitrogen-substituted tetraazaperopyrenes **12** and **13**, respectively (Scheme 4).

For the heteroatom-substituted tetraazaperopyrenes **10**–**13**, the position of the maximum of the absorption band varies dramatically (Figure 9). The phenoxy-substituted congener **10** displays an absorption maximum at 498 nm. The thiophenyl-substituted TAPP **11** (violet in solution) exhibits a significantly redshifted absorption band with a maximum at 565 nm, whereas the introduction of anilide substituents at the peropyrene core leads to TAPPs (**12**, **13**) that are blue in solution and are characterized by the bathochromic shift

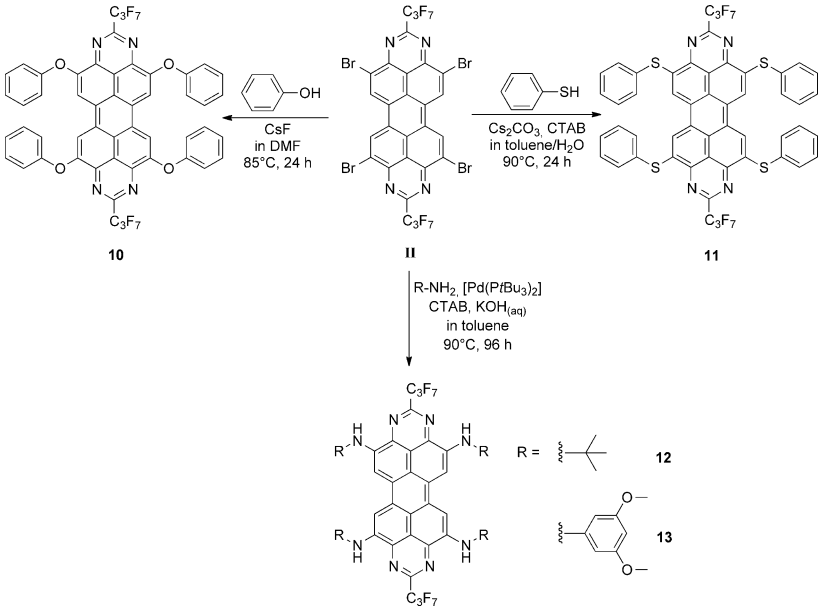

Scheme 4. Synthesis of the heteroatom-substituted TAPP derivatives **10**, **11**, **12**, and **13**.

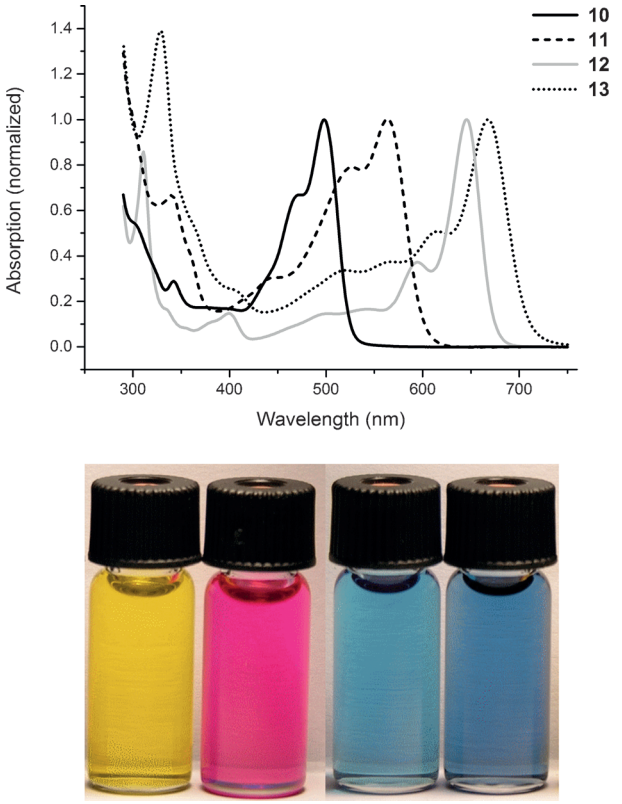

Figure 9. Normalized UV/Vis absorption spectra of the TAPP congeners **10**–**13** in THF (top) and the corresponding solutions seen in normal daylight. The introduction of heteroatoms leads to a bathochromic shift of the absorption band maxima.

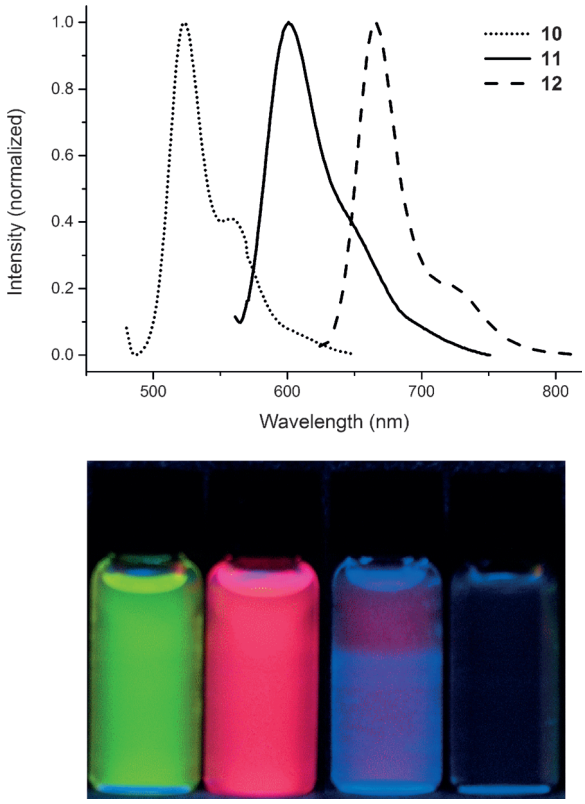

Figure 10. Normalized emission spectra of the tetraazaperopyrene derivatives **10**, **11**, and **12** in THF and the corresponding solutions of **10**, **11**, **12** (and **13**, which shows no emission) seen under laboratory UV light (λ_{ex} = 366 nm).

of the corresponding perylene band of about 100 nm compared to compound **11**. Overall, a spectral range of approximately 250 nm is covered by the π*←π bands of the four heteroatom-substituted TAPPs, as depicted in Figure 9.

Compounds **10**–**12** display much reduced emission quantum yields in THF compared to **1**–**7** (monoexponential fluorescence decay), whereas TAPP **13** shows no detectable fluorescence. For derivatives **11** and **12**, the emission maxima were observed at 606 and 666 nm, respectively, and are thus in the red region (compared to the characteristic green fluorescence of compounds **1**–**7**). Figure 10 shows the emission spectra of **10**, **11**, and **12** in THF, and the photophysical data for all the tetraazaperopyrene compounds are summarised in Table 5.

The O- and S-substituted derivatives **10** and **11** only exhibit reduction waves in the cyclic voltammograms, albeit at more negative potentials than **II**. This is more pronounced for the phenoxy derivative **10** because the greater electron affinity of sulfur compared to oxygen allows the reduction of compound **11** at slightly more positive potentials. Finally, substitution of the bromine atoms by nitrogen substituents leads to a dramatic shift of the reduction potentials, and for compounds **12** and **13**, reversible oxidation is also observed (Figure 11). This reversible redox wave is attributed to the formation of the cross-conjugated diimine species depicted in Figure 11. The electrochemical data for all new TAPP derivatives are summarised in Table 6.

Table 5. Summary of the photophysical data of the tetraazaperopyrene derivatives **II** and **10**–**13**.

	λ_{max} [nm] (log ε)	$\Delta\nu$ [cm^{-1}]	λ_{em} [nm] (Stokes shift)	Φ	τ [ns]
II	475 (4.91)	1419	486 (11)	0.12	2.1
10	498 (4.68)	1333	523 (25)	0.10	2.8
11	565 (4.58)	1276	606 (41)	0.06	0.5
12	646 (4.78)	1355	666 (20)	0.25	6.1
13	668 (4.59)	1264	–	–	–

Conclusion

Herein, we have presented the synthesis of several core-substituted tetraazaperopyrene derivatives starting from a fourfold brominated TAPP congener. Through subsequent substitution of the bromine atoms, it was possible to obtain fourfold phenyl- and alkynyl-substituted TAPP derivatives, as well as tetraazaperopyrenes with heteroatoms at the peropyrene core. Additionally, strong electron donors have been connected with the TAPP scaffold to give intramolecular donor–acceptor compounds.

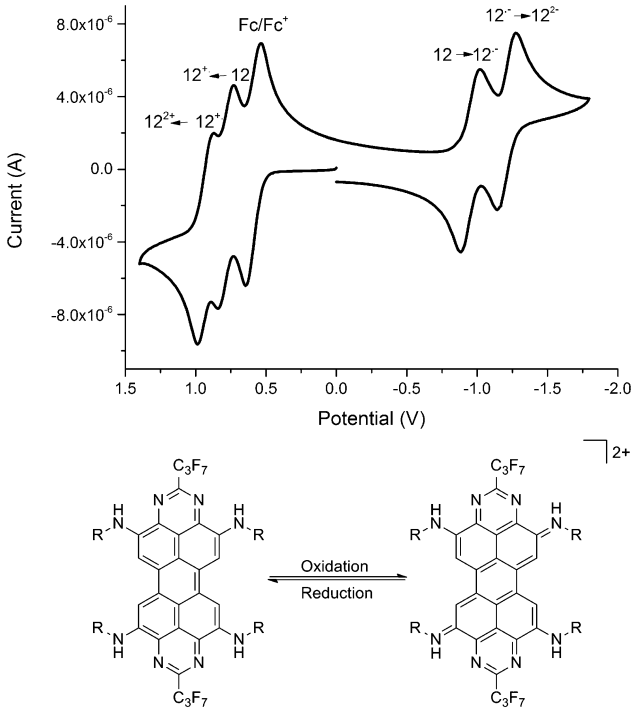

Figure 11. Cyclic voltammogram of **12** (top) and proposed oxidation (in two steps) to the diimine species (bottom).

Table 6. Summary of the electrochemical data derived from the cyclic voltammograms and DFT calculations.

	E_{Red1} [V][a]	E_{Red2} [V][a]	$E_{LUMO(CV)}$ [eV][b]	$E_{LUMO(DFT)}$ [eV][c]	E_{Ox} [V][a]	$E_{HOMO(CV)}$ [eV][b]	$E_{HOMO(DFT)}$ [eV][c]
II	−0.18	−0.56	−4.04	−4.10			−6.71
10	−0.47	−0.81	−3.74	−3.36			−5.94
11	−0.35	−0.67	−3.82	−3.49			−5.82
12	−0.95	−1.21	−3.26	−2.87	0.86	−5.00	−4.85
13	−0.71	−0.99	−3.51	−2.72	0.93	−5.14	−4.71

[a] **II**, **10**–**13**: Measured against SCF in THF. [b] Determined according to literature methods using Fc/Fc^+ as internal standard ($E_{HOMO}(Fc) = -4.8$ eV). [c] Calculated at the B3PW91/6–31 g(d,p) level of theory.

As expected, the substituents strongly enhance the solubility of these compounds in organic solvents, and the photophysical properties are influenced significantly by the different types of core substituents. Given the fact that a wide variety of substituents can be introduced to the aromatic core, it is now possible to cover the whole range of colours of the visible spectrum with TAPP derivatives. The emission properties are also affected by the different types of core substituents. The phenyl derivatives (**1**–**4**) display very high quantum yields of up to unity, and the emission wavelength could be shifted from around 510 nm (yellow/green) to approximately 660 nm (red) by introducing appropriate substituents.

With the methods in place for the core functionalization of TAPPs, it will be possible to tailor their properties for a range of applications. These include their use as biological fluorescence markers with specific binding properties and their applications in solar cells, the latter in particular for derivatives containing donor–acceptor units.

Experimental Section

The syntheses were performed under dried argon in standard Schlenk glassware, which was flame-dried prior to use. Solvents were dried according to standard procedures and saturated with argon. The ^1H and ^{13}C NMR spectra were recorded with Bruker AVANCE 400 and 600II$^+$ spectrometers equipped with variable-temperature units. Elemental analyses were performed in the Microanalytical Laboratory of the Chemistry Department at the University of Heidelberg. 2,9-bis-heptafluoropropyl-4,7,11,14-tetrachloro-1,3,8,10-tetraazaperopyrene (**I**)[10a] and 2,9-bis-heptafluoropropyl-4,7,11,14-tetrabromo-1,3,8,10-tetraazaperopyrene (**II**)[10b] were synthesised according to the literature procedures. All other starting materials were obtained commercially and used without further purification.

Preparation of 2,9-bis-(heptafluoropropyl)-4,7,11,14-tetrakis(phenyl)-1,3,8,10-tetraazaperopyrene (1): 2,9-Bis-(heptafluoropropyl)-4,7,11,14-tetrachloro-1,3,8,10-tetraazaperopyrene (**I**) (20 mg, 0.02 mmol), phenylboronic acid (20 mg, 0.16 mmol), KF (20 mg, 0.34 mmol), $[Pd_2(dba)_3]$ (2 mg, 0.002 mmol), and P(*t*Bu)$_3$ (1 mg, 0.005 mmol) were dissolved in 1,4-dioxane (10 mL) and heated to 100 °C for 9 days. The solvent was evaporated and the solid residue was extracted with chloroform. After evaporation of the solvent, the crude product was purified by column chromatography (silica, pentane/ethyl acetate 3:7). The solid was recrystallized from ethyl acetate, washed with methanol, and dried in vacuo. Yield: 10 mg (42 %, 0.1 mmol) of **1** as an orange solid. ^1H NMR (399.89 MHz, [D$_8$]THF): $\delta =$ 10.40 (s, 4H, C^{3}H), 8.26 (d, 8H, $^3J_{HH} = 7.1$ Hz, C^{9}H), 7.66 (t, 8H, $^3J_{HH} =$ 7.7 Hz, C^{10}H), 7.58 ppm (t, 4H, $^3J_{HH} = 7.4$ Hz, C^{11}H); ^{13}C NMR (150.9, [D$_8$]THF): $\delta = 154.5$ (C^1), 152.7 (m, C^7), 142.4 (C^2), 138.7 (C^8), 133.0 (C^3), 132.4 (C^9), 129.7 (C^{11}), 129.3 (C^{10}), 128.5 (C^4), 121.7 (C^5), 118.9 ppm (C^6), perfluorinated carbon atoms were not detected at the attainable S/N ratio; ^{19}F NMR (376.27 MHz, [D$_8$]THF): $\delta = -81.12$ (t, 6F, $^3J_{FF} = 9.3$ Hz, CF_3), −113.71 (q, 4F, $^3J_{FF} = 9.2$ Hz, CF_2), −126.10 ppm (s, 4F, CF_2); HR-MS (FAB$^+$): *m/z* calcd for $C_{52}H_{25}F_{14}N_4$: 971.1856; found: 971.1839.

General procedure A for the preparation of fourfold phenyl-substituted tetraazaperopyrene derivatives starting from compound II: 2,9-Bis-(heptafluoropropyl)-4,7,11,14-tetrabromo-1,3,8,10-tetraazaperopyrene (**II**) (100 mg, 0.10 mmol), [Pd(dppf)Cl$_2$] (7.3 mg, 0.01 mmol), Cs_2CO_3 (228 mg, 0.70 mmol), and the corresponding phenylboronic acid (0.6 mmol) were dissolved in 1,4-dioxane (25 mL). The resulting mixture was heated to 100 °C for 48 h. Then, the mixture was dispersed on celite and purified by column chromatography (silica, pentane/ethyl acetate 2:1). The solid product was washed with methanol and pentane and dried in vacuo.

2,9-Bis-(heptafluorpropyl)-4,7,11,14-tetrakis(4-cyanophenyl)-1,3,8,10-tetraazaperopyrene (2): Synthesised according to general procedure **A** with 4-cyanophenylboronic acid. Yield: 22 mg (20 %, 0.02 mmol) of **2** as an orange solid ($R_f = 0.85$). ^1H NMR (600.13 MHz, [D$_8$]THF): $\delta = 10.53$ (s, 4H, C^{3}H), 8.43 (d, 8H, $^3J_{HH} = 7.9$ Hz, C^{9}H), 8.09 ppm (d, 8H, $^3J_{HH} =$ 7.9 Hz, C^{10}H); ^{13}C NMR (150.92 MHz, [D$_8$]THF): $\delta = 154.2$ (C^1), 142.6 (C^2), 140.8 (C^8), 134.2 (C^3), 133.2 (C^9), 133.1 (C^{10}), 128.9 (C^4), 122.3 (C^5), 119.4 (C^{12}), 114.2 ppm (C^{11}), perfluorinated carbon atoms, C6 and C7 were not detected at the attainable S/N ratio; ^{19}F NMR (376.27 MHz, [D$_8$]THF): $\delta = -81.10$ (t, 6F, $^3J_{FF} = 9.3$ Hz, CF_3), −113.87 (m, 4F, CF_2), −126.07 ppm (m, 4F, CF_2); HR-MS (MALDI$^+$): *m/z* calcd for $C_{56}H_{21}F_{14}N_8$: 1071.1660; found: 1071.1649.

2,9-Bis-(heptafluoropropyl)-4,7,11,14-tetrakis(4-trifluoromethylphenyl)-1,3,8,10-tetraazaperopyrene (3): Synthesised according to general procedure **A** with 4-trifluoromethylphenylboronic acid. Yield: 80 mg (60 %, 0.06 mmol) of **3** as an orange solid ($R_f = 0.88$). ^1H NMR (600.13 MHz, [D$_8$]THF): $\delta = 10.52$ (s, 4H, C^{3}H), 8.47 (d, 8H, $^3J_{HH} = 7.9$ Hz, C^{9}H), 8.04 ppm (d, 8H, $^3J_{HH} = 8.3$ Hz, C^{10}H); ^{13}C NMR (150.92 MHz, [D$_8$]THF): $\delta = 152.9$ (C^1), 141.0 (C^8), 139.7 (C^2), 132.9 (C^3), 131.8 (C^9), 130.4 (q, $^2J_{CF} = 31.9$ Hz, C^{11}), 127.5 (C^4), 125.0 (q, $^3J_{CF} = 3.7$ Hz, C^{10}), 124.5 (q, $^1J_{CF} = 271.4$ Hz, C$^{12}F_3$), 120.9 (C^5), 117.5 ppm (C^6), perfluorinated

carbon atoms and C7 were not detected at the attainable S/N ratio; ^{19}F NMR (376.27 MHz, [D$_8$]THF): $\delta = -63.23$ (s, 12F, C^{12}F$_3$), -81.08 (t, 6F, $^3J_{FF} = 9.2$ Hz, CF$_3$), -113.78 (m, 4F, CF$_2$), -126.03 ppm (m, 4F, CF$_2$); HR-MS (MALDI$^+$): *m/z* calcd for $C_{56}H_{21}F_{26}N_4$: 1242.1268; found: 1242.1246; elemental analysis calcd (%) for $C_{56}H_{20}F_{26}N_4$: C 54.12, H 1.62, N 4.51; found: C 53.94, H 1.92, N 4.48.

2,9-Bis-(heptafluoropropyl)-4,7,11,14-tetrakis(4-carboxyethylphenyl)-1,3,8,10-tetraazaperopyrene (4): Synthesised according to general procedure **A** with 4-carboxyethylphenylboronic acid. Yield: 105 mg (84%, 0.08 mmol) of **4** as an orange solid ($R_f = 0.85$). ^{1}H NMR (600.13 MHz, CDCl$_3$): $\delta = 9.96$ (s, 4H, C^{3}H), 8.37 (d, 8H, $^3J_{HH} = 7.9$ Hz, C^{10}H), 8.22 (d, 8H, $^3J_{HH} = 7.9$ Hz, C^{9}H), 4.51 (q, 8H, $^3J_{HH} = 7.1$ Hz, C^{13}H$_2$), 1.51 ppm (t, 12H, $^3J_{HH} = 7.1$ Hz, C^{14}H$_3$); ^{13}C NMR (150.92 MHz, CDCl$_3$): $\delta = 166.6$ (C^{12}), 153.7 (t, $^2J^{CF} = 26.3$ Hz, C^7), 152.8 (C^1), 140.9 (C^8), 140.6 (C^{11}), 131.1 (C^3), 131.0 (C^9), 130.9 (C^2), 129.7 (C^{10}), 126.6 (C^4), 120.6 (C^5), 117.2 (C^6), 61.3 (C^{13}), 14.4 ppm (C^{14}), perfluorinated carbon atoms were not detected at the attainable S/N ratio; ^{19}F NMR (376.27 MHz, CDCl$_3$): $\delta = -80.09$ (t, 6F, $^3J_{FF} = 8.9$ Hz, CF$_3$), -113.56 (m, 4F, CF$_2$), -125.44 ppm (m, 4F, CF$_2$); HR-MS (MALDI$^+$): *m/z* calcd for $C_{64}H_{41}F_{14}O_8N_4$: 1259.2701; found: 1259.2695; elemental analysis calcd (%) for $C_{64}H_{40}F_{14}O_8N_4$: C 61.06, H 3.20, N 4.45; found: C 60.18, H 3.36, N 4.44.

2,9-Bis-(heptafluoropropyl)-4,7,11,14-tetrakis((*tert*-butyldimethylsilyl)ethinyl)-1,3,8,10-tetraazaperopyrene (5): 2,9-Bis-(heptafluoropropyl)-4,7,11,14-tetrabromo-1,3,8,10-tetraazaperopyrene (**II**) (100 mg, 0.10 mmol), [Pd(dppf)Cl$_2$] (15 mg, 0.02 mmol), Cs_2CO_3 (260 mg, 0.80 mmol), and 2-((*tert*-butyldimethylsilyl)ethynyl)boronic acid pinacol ester (160 mg, 0.6 mmol) were dissolved in 1,4-dioxane (25 mL) and heated to 100°C for 72 h. The solvent was evaporated, and the solid residue was washed with methanol as well as pentane and dried in vacuo. Yield: 40 mg (33%, 0.03 mmol) of **4** as a dark red solid. ^{1}H NMR (600.13 MHz, [D$_8$]THF): $\delta = 10.40$ (s, 4H, C^{3}H), 1.21 (s, 36H, (C^{12}H$_3$)$_3$), 0.39 ppm (s, 24H, C^{10}H$_3$); ^{13}C NMR (150.92 MHz, [D$_8$]THF): $\delta = 155.5$ (C^1), 137.7 (C^3), 128.5 (C^4), 125.6 (C^2), 121.6 (C^5), 117.6 (C^6), 105.4 (C^9), 102.6 (C^8), 26.8 (C^{12}), 17.9 (C^{11}), -4.2 ppm (C^{10}), perfluorinated carbon atoms and C7 were not detected at the attainable S/N ratio; ^{19}F NMR (376.27 MHz, [D$_8$]THF): $\delta = -81.10$ (t, 6F, $^3J_{FF} = 9.0$ Hz, CF$_3$), -113.67 (m, 4F, CF$_2$), -126.04 ppm (m, 4F, CF$_2$); ^{29}Si NMR (79.4 MHz, [D$_8$]THF): $\delta = -6.66$ ppm; HR-MS (MALDI$^+$): *m/z* calcd for $C_{60}H_{64}F_{14}N_4Si_4$ 1218.3979; found: 1218.3937; elemental analysis calcd (%) for $C_{60}H_{64}F_{14}N_4Si_4{\cdot}CH_3OH$: C 58.54, H 5.48, N 4.48; found: C 58.28, H 5.40, N 4.45.

2,9-Bis-(heptafluoropropyl)-4,7,11,14-tetrakis(trimethylsilylethinyl)-1,3,8,10-tetraazaperopyrene (6): [Pd(P(*t*Bu)$_3$)$_2$] (12 mg, 0.024 mmol), 2,9-bis-(heptafluoropropyl)-4,7,11,14-tetrabromo-1,3,8,10-tetraazaperopyrene (**II**) (200 mg, 0.20 mmol), and Cs_2CO_3 (586 mg, 1.80 mmol) were dissolved in 1,4-dioxane (20 mL), and trimethyl((tributylstannyl)ethynyl)-silane[20] (465 mg, 1.20 mmol) was added dropwise. The reaction mixture was heated to 80°C for 24 h and filtered through celite, and the celite pad was washed with diethyl ether. The solvent was evaporated, and the solid residue was washed with methanol and pentane and dried in vacuo. Yield: 120 mg (57%, 0.11 mmol) of **5** as a dark red solid. ^{1}H NMR (600.13 MHz, [D$_8$]THF): $\delta = 10.37$ (s, 4H, C^{3}H), 0.40 ppm (s, 36H, C^{10}H$_3$); ^{13}C NMR (150.92 MHz, [D$_8$]THF): $\delta = 154.0$ (C^1), 150.1 (C^7), 136.0 (C^3), 127.2 (C^4), 124.3 (C^2), 120.4 (C^5), 116.2 (C^6), 105.5 (C^9), 100.5 (C^8), -1.2 ppm (C^{10}), perfluorinated carbon atoms were not detected at the attainable S/N ratio; ^{19}F NMR (376.27 MHz, [D$_8$]THF): $\delta = -80.91$ (t, 6F, $^3J_{FF} = 8.9$ Hz, CF$_3$), -113.28 (m, 4F, CF$_2$), -125.88 ppm (m, 4F, CF$_2$); ^{29}Si NMR (79.4 MHz, [D$_8$]THF): $\delta = -16.32$ ppm; HR-MS (MALDI$^+$): *m/z* calcd for $C_{48}H_{41}F_{14}N_4Si_4$: 1051.2179; found: 1051.2135; elemental analysis calcd (%) for $C_{48}H_{40}F_{14}N_4Si_4$: C 54.84, H 3.84, N 5.33; found: C 54.37, H 3.91, N 5.18.

2,9-Bis-(heptafluoropropyl)-4,7,11,14-tetrakis(triisopropylsilylethinyl)-1,3,8,10-tetraazaperopyrene (7): [Pd(dppf)Cl$_2$] (15 mg, 0.02 mmol), CuI (15 mg, 0.08 mmol), and 2,9-bis-(heptafluoropropyl)-4,7,11,14-tetrabromo-1,3,8,10-tetraazaperopyrene (**II**) (100 mg, 0.10 mmol) were dissolved in THF (15 mL) and NEt$_3$ (5 mL). Triisopropylsilylacetylene (474 mg, 2.60 mmol) was added slowly and the reaction mixture was stirred at room temperature for 10 min. The reaction mixture was filtrated over celite and the celite pad was washed with pentane. Then, the raw product was dispersed on celite and purified by column chromatography (silica, pentane/ethyl acetate 9:1). The solvent was evaporated and the solid was washed with methanol, acetonitrile, and hexamethyldisiloxane. Yield: 110 mg (80%, 0.08 mmol) of **7** as a dark red solid ($R_f = 0.87$). ^{1}H NMR (600.13 MHz, [D$_8$]THF): $\delta = 10.41$ (s, 4H, C^{3}H), 1.35 ppm (s, 84H, C^{11}H$_3$); ^{13}C NMR (150.92 MHz, [D$_8$]THF): $\delta = 154.4$ (C^1), 135.9 (C^3), 127.2 (C^4), 124.4 (C^2), 120.4 (C^5), 116.5 (C^6), 102.7 (C^9), 102.5 (C^8), 18.2 (C^{11}), 11.5 ppm (C^{10}), perfluorinated carbon atoms and C7 were not detected at the attainable S/N ratio; ^{19}F NMR (376.27 MHz, [D$_8$]THF): $\delta = -81.14$ (t, 6F, $^3J_{FF} = 9.0$ Hz, CF$_3$), -113.68 (m, 4F, CF$_2$), -125.93 ppm (m, 4F, CF$_2$); ^{29}Si NMR (79.4 MHz, [D$_8$]THF): $\delta = -0.66$ ppm; HR-MS (MALDI$^+$): *m/z* calcd for $C_{72}H_{89}F_{14}N_4Si_4$: 1387.5938; found: 1387.5935.

2,9-Bis-(heptafluoropropyl)-4,7,11,14-tetrakis(1-pyrenyl)-1,3,8,10-tetra-azaperopyrene (8): 2,9-Bis-(heptafluoropropyl)-4,7,11,14-tetrabromo-1,3,8,10-tetraazaperopyrene (**II**) (200 mg, 0.2 mmol), pyrene-2-boronic acid (394 mg, 0.8 mmol), Cs_2CO_3 (652 mg, 2.0 mmol), [Pd$_2$(dba)$_3$] (18 mg, 0.02 mmol), and P(*t*Bu)$_3$ (8 mg, 0.04 mmol) were dissolved in 1,4-dioxane (30 mL) and heated to 100°C for 96 h. The reaction mixture was dispersed on celite and purified by column chromatography (silica, pentane/ethyl acetate 2:1). The solvent was evaporated, and the solid was washed with methanol and pentane and dried in vacuo. Yield: 190 mg (64%, 0.13 mmol) of **8** as a dark green solid ($R_f = 0.65$). ^{1}H NMR (600.13 MHz, [D$_8$]THF): $\delta = 10.36$ (s, 4H, C^{3}H), 8.52–7.91 ppm (m, 36H, pyrene-H); ^{13}C NMR (150.92 MHz, [D$_8$]THF): $\delta = 155.6$ (C^1), 143.8 (C^2), 135.8 (C^3), 134.0 (C^8), 132.7 (C^q), 132.3 (C^q), 131.7 (C^q), 130.5 (C^{pyrene}-H), 129.1 (C^{pyrene}-H), 128.6 (C^{pyrene}-H), 128.5 (C^{pyrene}-H), 127.2 (C^{pyrene}-H), 126.6 (C^{pyrene}-H), 126.3 (C^{Pyrene}-H), 126.0 (C^q), 125.9 (C^q), 125.5 ppm (C^{pyrene}-H), perfluorinated carbon atoms and C7 were not detected at the attainable S/N ratio; ^{19}F NMR (376.27 MHz, [D$_8$]THF): $\delta = -81.21$ (t, 6F, $^3J_{FF} = 8.9$ Hz, CF$_3$), -113.98 (m, 4F, CF$_2$), -126.26 ppm (m, 4F, CF$_2$); HR-MS (MALDI$^+$): *m/z* calcd for $C_{92}H_{40}F_{14}N_4$: 1466.3029; found: 1466.3032; elemental analysis calcd (%) for $C_{92}H_{40}F_{14}N_4{\cdot}CH_3OH$: C 74.50, H 2.96, N 3.74; found: C 74.10, H 3.08, N 3.77.

2,9-Bis-(heptafluorepropyl)-4,7,11,14-tetrakis(4-(diphenylamino)phenyl)-1,3,8,10-tetraazaperopyrene (9): 2,9-Bis-(heptafluoropropyl)-4,7,11,14-tetrabromo-1,3,8,10-tetraazaperopyrene (**II**) (100 mg, 0.1 mmol), 4-(diphenylamino)-phenylboronic acid (174 mg, 0.6 mmol), Cs_2CO_3 (228 mg, 0.7 mmol), [Pd$_2$(dba)$_3$] (10 mg, 0.01 mmol), and P(*t*Bu)$_3$ (4 mg, 0.02 mmol) were dissolved in 1,4-dioxane (20 mL) and the reaction mixture was heated to 100°C for 72 h. The reaction mixture was filtrated over celite, and the raw product was dispersed on celite and purified by column chromatography (silica, pentane/ethyl acetate 2:1). The solvent was evaporated and the solid residue was washed with methanol and pentane. Yield: 85 mg (51%, 0.05 mmol) of **9** as a dark green solid ($R_f = 0.83$). ^{1}H NMR (600.13 MHz, [D$_8$]THF): $\delta = 10.27$ (s, 4H, C^{3}H), 8.20 (d, 8H, $^3J_{HH} = 8.4$ Hz, C^{9}H), 7.33–7.31 (m, 24H, C^{10}H and C^{14}H), 7.24 (d, 16H, $^3J_{HH} = 7.6$ Hz, C^{13}H), 7.09 ppm (t, 8H, $^3J_{HH} = 7.3$ Hz, C^{15}H); ^{13}C NMR (150.92 MHz, [D$_8$]THF): $\delta = 154.4$ (C^1), 149.8 (C^{11}), 148.9 (C^{12}), 141.1 (C^2), 134.6 (C^8), 133.4 (C^9), 132.1 (C^3), 130.6 (C^{14}), 128.2 (C^4), 126.2 (C^{13}), 124.6 (C^{15}), 123.4(C^{10}), 121.2 (C^5), 118.9 ppm (C^6), perfluorinated carbon atoms and C7 were not detected at the attainable S/N ratio; ^{19}F NMR (376.27 MHz, [D$_8$]THF): $\delta = -81.21$ (t, 6F, $^3J_{FF} = 8.9$ Hz, CF$_3$), -113.98 (m, 4F, CF$_2$), -126.26 ppm (m, 4F, CF$_2$); HR-MS (MALDI$^+$): *m/z* calcd for $C_{100}H_{60}F_{14}N_8$: 1638.4712; found: 1638.4719; elemental analysis calcd (%) for $C_{100}H_{60}F_{14}N_8{\cdot}CH_3OH$: C 72.57, H 3.86, N 6.70; found: C 72.12, H 4.02, N 6.85.

2,9-Bis-(heptafluoropropyl)-4,7,11,14-tetrakis(phenoxy)-1,3,8,10-tetraaza-peropyrene (10): DMF (20 mL) was added to a mixture of 2,9-bis-(heptafluoropropyl)-4,7,11,14-tetrabromo-1,3,8,10-tetraazaperopyrene (**II**) (100 mg, 0.10 mmol), CsF (152 mg, 1.0 mmol), and phenol (75 mg, 0.8 mmol), and the resulting reaction mixture was heated to 90°C for 24 h. Aqueous hydrochloric acid was added until no further solid precipitated. The red precipitate was collected by filtration, washed with water, methanol, and pentane, and dried in vacuo. Yield: 60 mg (60%, 0.06 mmol) of **10** as a red solid. ^{1}H NMR (600.13 MHz, [D$_8$]THF): $\delta = 9.26$ (s, 4H, C^{3}H), 7.44 (t, 8H, $^3J_{HH} = 8.0$ Hz, C^{10}H), 7.29–7.25 ppm (m, 12H, C^{9}H and C^{10}H); ^{13}C NMR (150.92 MHz, [D$_8$]THF): $\delta = 158.5$ (C^8),

154.0 (C^1), 150.3 (C^2), 131.3 (C^{10}), 127.8 (C^4), 125.5 (C^{11}), 120.2 (C^9), 118.7 (C^3), 117.2 ppm (C^5), perfluorinated carbon atoms, C6 and C7 were not detected at the attainable S/N ratio; ^{19}F NMR (376.27 MHz, [D$_8$]THF): $\delta = -81.19$ (t, 6F, $^3J_{FF} = 9.2$ Hz, CF_3), -113.63 (m, 4F, CF_2), -126.17 ppm (m, 4F, CF_2); (MALDI$^+$): *m/z* calcd for $C_{52}H_{24}F_{14}N_4O_4$: 1034.1557; found: 1034.1568.

2,9-Bis-(heptafluoropropyl)-4,7,11,14-tetrakis(thiophenyl)-1,3,8,10-tetraazaperopyrene (11): Toluene (40 mL) and water (10 mL) were added to a mixture of 2,9-bis-(heptafluoropropyl)-4,7,11,14-tetrabromo-1,3,8,10-tetraazaperopyrene (**II**) (100 mg, 0.10 mmol), Cs_2CO_3 (650 mg, 2.0 mmol), and CTAB (36 mg, 0.1 mmol). Thiophenol (0.1 mL, 0.1 mmol) was added dropwise and the reaction mixture was heated to 90 °C for 24 h. The reaction mixture was extracted with chloroform, and the organic layer was washed with brine and dried over Na_2SO_4. The solvent was evaporated and the solid residue was washed with methanol and pentane. Yield: 117 mg (54 %, 0.11 mmol) of **10** as a red solid. ^{1}H NMR (600.13 MHz, [D$_8$]THF): $\delta = 8.92$ (s, 4H, C^3H), 7.71 (d, 8H, $^3J_{HH} = 7.2$ Hz, C^9H), 7.53 (d, 8H, $^3J_{HH} = 7.6$ Hz, C^{10}H), 7.06 ppm (t, 4H, $^3J_{HH} = 7.5$ Hz, C^{11}H); ^{13}C NMR (150.92 MHz, [D$_8$]THF): $\delta = 153.0$ (C^1), 142.5 (C^2), 135.0 (C^9), 131.8 (C^8), 131.0 (C^{10}), 130.8 (C^{11}), 127.4 (C^3), 127.1 (C^4), 119.3 (C^5), 117.8 ppm (C^6), perfluorinated carbon atoms and C7 were not detected at the attainable S/N ratio; ^{19}F NMR (376.27 MHz, [D$_8$]THF): $\delta = -81.02$ (t, 6F, $^3J_{FF} = 8.9$ Hz, CF_3), -113.66 (m, 4F, CF_2), -126.05 ppm (m, 4F, CF_2); HR-MS (FAB$^+$): *m/z* calcd for $C_{52}H_{25}F_{14}N_4S_4$: 1099.0738; found: 1099.0753.

2,9-Bis-(heptafluoropropyl)-4,7,11,14-tetrakis(3,5-dimethoxyaniline)-1,3,8,10-tetraazaperopyrene (13): Toluene (15 mL) was added to a mixture of 2,9-bis-(heptafluoropropyl)-4,7,11,14-tetrabromo-1,3,8,10-tetraazaperopyrene (**II**) (100 mg, 0.10 mmol), [Pd(P(*t*Bu)$_3$)$_2$] (15 mg, 0.03 mmol), and CTAB (18 mg, 0.05 mmol). 3,5-Dimethoxyaniline (92 mg, 0.6 mmol) and KOH (45 mg, 0.8 mmol, in 0.5 mL H_2O) were added to this mixture, and the resulting reaction mixture was heated to 90 °C for 96 h. Then, it was filtrated through celite, and the raw product was purified by column chromatography (silica, pentane/ethyl acetate 9:1). The solvent was evaporated, and the solid residue was washed with methanol and hexamethyldisiloxane and dried in vacuo. Yield: 46 mg (36 %, 0.04 mmol) of **13** as a blue solid. ^{1}H NMR (600.13 MHz, [D$_8$]THF): $\delta = 9.37$ (s, 4H, C^3H), 8.54 (s, 4H, NH), 6.85 (s, 8H, C^9H), 6.40 (s, 4H, C^{11}H), 3.76 ppm (s, 24H, $OC^{12}H_3$); ^{13}C NMR (150.92 MHz, [D$_8$]THF): $\delta = 163.4$ (C^{10}), 147.8 (C^1), 143.3 (C^8), 139.0 (C^4), 126.4 (C^2), 117.8 (C^6), 112.7 (C^5), 107.6 (C^3), 100.2 (C^9), 97.7 (C^{11}), 55.9 ppm (C^{12}), perfluorinated carbon atoms and C7 were not detected at the attainable S/N ratio; ^{19}F NMR (376.27 MHz, [D$_8$]THF): $\delta = -80.97$ (t, 6F, $^3J_{FF} = 9.1$ Hz, CF_3), -113.83 (m, 4F, CF_2), -125.80 ppm (m, 4F, CF_2); HR-MS (MALDI$^+$): *m/z* calcd for $C_{60}H_{44}F_{14}N_4O_8$: 1270.3017; found: 1270.3053.

2,9-Bis-(heptafluoropropyl)-4,7,11,14-tetrakis(*tert*-butylamino)-1,3,8,10-tetraazaperopyrene (12): Toluene (15 mL) was added to a mixture of 2,9-bis-(heptafluoropropyl)-4,7,11,14-tetrabromo-1,3,8,10-tetraazaperopyrene (**II**) (100 mg, 0.10 mmol), Pd(P(*t*Bu)$_3$)$_2$ (15 mg, 0.03 mmol), and CTAB (18 mg, 0.05 mmol). Then, *tert*-butylamine (0.2 mL, 2.0 mmol) and KOH (45 mg, 0.8 mmol, in 0.5 mL H_2O) were added and the reaction mixture was heated to 90 °C for 96 h. The raw product was filtrated through celite and purified by column chromatography (silica, pentane/ethyl acetate 9:1). The solvent was evaporated, and the solid residue washed with methanol and hexamethyldisiloxane and dried in vacuo. Yield: 32 mg (34 %, 0.03 mmol) of **12** as a blue solid. ^{1}H NMR (600.13 MHz, [D$_8$]THF): $\delta = 8.77$ (s, 4H, C^3H), 6.67 (s, 4H, NH), 1.83 ppm (s, 36H, C^9H); ^{13}C NMR (150.92 MHz, [D$_8$]THF): $\delta = 148.1$ (C^1), 140.6 (C^2), 125.7 (C^4), 117.9 (C^6), 110.6 (C^5), 106.4 (C^3), 52.3 (C^8), 29.9 ppm (C^9), perfluorinated carbon atoms and C7 were not detected at the attainable S/N ratio; ^{19}F NMR (376.27 MHz, [D$_8$]THF): $\delta = -80.81$ (t, 6F, $^3J_{FF} = 9.0$ Hz, CF_3), -113.48 (m, 4F, CF_2), -125.88 ppm (m, 4F, CF_2); HR-MS (MALDI$^+$): *m/z* calcd for $C_{44}H_{44}F_{14}N_8$: 950.3448; found: 950.3459; elemental analysis calcd (%) for $C_{44}H_{44}F_{14}N_8 \cdot CH_3OH$: C 54.99, H 4.92, N 11.40; found: C 54.43, H 4.91, N 10.91.

Photophysical measurements: The UV/Vis absorption spectra were recorded on a Cary 5000 UV/Vis/NIR spectrophotometer and were baseline- and solvent-corrected. Emission spectra were recorded on a Varian Cary Eclipse Spectrophotometer and standard corrections were applied to all spectra. Fluorescence lifetimes were determined on a Fluotime 100 Fluorescence Lifetime System equipped with a PDL 800-D picosecond pulsed laser unit. The goodness of fit was assessed by minimizing the reduced chi squared function (χ^2) and visual inspection of the weighted residuals. Fluorescence spectra and luminescence quantum yields (Φ) were measured on a Varian Cary Eclipse Spectrophotometer. Luminescence quantum yields (Φ) were determined in optically dilute solutions (O.D. < 0.05 at excitation wavelength) and compared to reference emitters by using Equation (1),[21] in which A is the absorbance at the excitation wavelength (λ), I is the intensity of the excitation light at the excitation wavelength (λ), n is the refractive index of the solvent, D is the integrated intensity of the luminescence, and Φ is the quantum yield. The subscripts r and x refer to the reference and the sample, respectively. All quantum yields were measured at identical excitation wavelengths for the sample and the reference, cancelling the $I(\lambda_r)/I(\lambda_x)$ term in the equation.

$$\Phi_x = \Phi_r \left[\frac{A_r(\lambda_r)}{A_x(\lambda_x)}\right]\left[\frac{I_r(\lambda_r)}{I_x(\lambda_x)}\right]\left[\frac{n_x^2}{n_r^2}\right]\left[\frac{D_x}{D_r}\right] \quad (1)$$

For determination of the quantum yields of the discussed samples in THF, either an aqueous solution (0.1 M NaOH) of fluorescein ($\Phi = 0.87$; **1**–**7**, **10**)[22] was used or a solution of cresyl violet perchlorate in ethanol ($\Phi = 0.54$; **11**–**13**).[23] The solvents for spectroscopic studies were of spectroscopic grade and used as received.

Cyclic voltammetry: Cyclic voltammetry was performed with a standard commercial electrochemical analyzer in a three-electrode single-component cell under argon. A platinum disk was used as the working electrode, a platinum wire as the counter electrode, and a saturated calomel electrode as the reference electrode. All potentials were internally referenced to ferrocene. THF or CH_2Cl_2 were used as solvents, which were dried and degassed prior to measurement. The supporting electrolyte was 0.1 M tetrabutylammonium hexafluorophosphate. The measurements were made under the exclusion of air and moisture.

Computational studies: The DFT-B3PW91 functional was employed to model the systems in this work with a 6–31 g(d,p) basis set for all atoms.[24] All the calculations were performed with the GAUSSIAN03 program package.[25] Every geometry optimization was followed by a frequency analysis to verify the energy minima. Electron affinities were determined by optimizing the structure of the anionic species by using the previously optimized geometry of the neutral species as the input and taking the difference of the total energies of both species.

Crystal data of 6: $C_{48}H_{40}F_{14}N_4Si_4$; monoclinic; space group $P2_1/c$; $a = 6.2619(2)$, $b = 13.6801(5)$, $c = 30.8928(10)$ Å; $\beta = 93.959(3)°$; $V = 2640.1(2)$ Å^3; $Z = 2$; $\mu = 1.809$ mm^{-1}; $F_{000} = 1076$; $T = 115(2)$ K; θ range 3.5° to 72.0°; index ranges h, k, l: $-7\ldots7$, $-16\ldots16$, $-37\ldots37$; reflections measured: 40974; independent: 5148 [$R_{int} = 0.103$]; observed [$I > 2\sigma(I)$]: 4163; final R indices [$F_o > 4\sigma(F_o)$]: $R(F) = 0.0953$; $wR(F^2) = 0.2261$; $GooF = 1.117$. Data collection: Agilent Technologies Supernova-E CCD diffractometer, $Cu_{K\alpha}$ radiation, microfocus X-ray tube, multilayer mirror optics, $\lambda = 1.5418$ Å. Lorentz, polarization, and numerical absorption correction.[26] Structure solution: charge flip procedure.[27] Refinement: full-matrix least squares methods based on F^2;[28] all non-hydrogen atoms anisotropic, hydrogen atoms at calculated positions (refined riding). CCDC-932410 contains the supplementary crystallographic data for this paper. These data can be obtained free of charge from The Cambridge Crystallographic Data Centre via www.ccdc.cam.ac.uk/data_request/cif.

Acknowledgements

We gratefully acknowledge funding of this work by the project "Polytos", which is embedded in the leading edge cluster "Forum Organic Electronics" (FKZ 13N10205). We thank Danuta Gutruf for carrying out the cyclic voltammetric studies, Beate Termin for help in recording ^{13}C NMR spectra of highly dilute solutions, and Dr. Matthias Kruck and Prof.

Markus Enders for advice in connection with the DFT modelling of the molecular properties.

[1] Selected reviews: a) H. Langhals, *Heterocycles* **1995**, *40*, 477; b) F. Würthner, *Chem. Commun.* **2004**, 1564; c) C. Huang, S. Barlow, S. R. Marder, *J. Org. Chem.* **2011**, *76*, 2386; d) C. Li, H. Wonneberger, *Adv. Mater.* **2012**, *24*, 613.

[2] Reviews: a) F. Würthner, M. Stolte, *Chem. Commun.* **2011**, *47*, 5109; b) J. E. Anthony, A. Facchetti, M. Heeney, S. R. Marder, X. Zhan, *Adv. Mater.* **2010**, *22*, 3876.

[3] Selected references: a) J. G. Laquindanum, H. E. Katz, A. Dodabalapur, A. J. Lovinger, *J. Am. Chem. Soc.* **1996**, *118*, 11331; b) S. K. Lee, Y. Zu, A. Herrmann, Y. Geerts, K. Müllen, A. J. Bard, *J. Am. Chem. Soc.* **1999**, *121*, 3513; c) H. Quante, K. Müllen, *Angew. Chem.* **1995**, *107*, 1487; *Angew. Chem. Int. Ed. Engl.* **1995**, *34*, 1323; d) L. Schmidt-Mende, A. Fechtenkötter, K. Müllen, E. Moons, R. H. Friend, J. D. MacKenzie, *Science* **2001**, *293*, 1119; e) M. J. Ahrens, M. J. Fuller, M. R. Wasielewski, *Chem. Mater.* **2003**, *15*, 2684; f) B. A. Jones, M. J. Ahrens, M.-H. Yoon, A. Facchetti, T. J. Marks, M. R. Wasielewski, *Angew. Chem.* **2004**, *116*, 6523; *Angew. Chem. Int. Ed.* **2004**, *43*, 6363; g) X. Zhan, Z. A. Tan, B. Domercq, Z. An, X. Zhang, S. Barlow, Y. Li, D. Zhu, B. Kippelen, S. R. Marder, *J. Am. Chem. Soc.* **2007**, *129*, 7246; h) S. M. Lindner, N. Kaufmann, M. Thelakkat, *Org. Electron.* **2007**, *8*, 69; i) C. Liu, Z. Liu, H. T. Lemke, H. N. Tsao, R. C. G. Naber, Y. Li, K. Banger, K. Müllen, M. M. Nielsen, H. Sirringhaus, *Chem. Mater.* **2010**, *22*, 2120; j) M. Gsänger, J. H. Oh, M. Könemann, H. W. Höffken, A.-M. Krause, Z. Bao, F. Würthner, *Angew. Chem.* **2010**, *122*, 752; *Angew. Chem. Int. Ed.* **2010**, *49*, 740.

[4] Selected key references: a) G. Seybold, G. Wagenblast, *Dyes Pigm.* **1989**, *11*, 303; b) B. Rybtchinski, L. E. Sinks, M. R. Wasielewski, *J. Am. Chem. Soc.* **2004**, *126*, 12268; c) F. Würthner, *Pure Appl. Chem.* **2006**, *78*, 2341; d) R. F. Kelley, W. S. Shin, B. Rybtchinski, L. E. Sinks, M. R. Wasielewski, *J. Am. Chem. Soc.* **2007**, *129*, 3173; e) A. J. Jiménez, F. Spänig, M. S. Rodríguez-Morgade, K. Ohkubo, S. Fukuzumi, D. M. Guldi, T. Torres, *Org. Lett.* **2007**, *9*, 2481; f) K. Peneva, G. Mihov, F. Nolde, S. Rocha, J. Hotta, K. Braeckmans, J. Hofkens, H. Uji-I, A. Herrmann, K. Müllen, *Angew. Chem.* **2008**, *120*, 3420; *Angew. Chem. Int. Ed.* **2008**, *47*, 3372; g) J. Baffreau, S. Leroy-Lhez, V. A. Nguyen, R. M. Williams, P. Hudhomme, *Chem. Eur. J.* **2008**, *14*, 4974; h) R. Schmidt, J. H. Oh, Y. S. Sun, M. Deppisch, A. M. Krause, K. Radacki, H. Braunschweig, M. Könemann, P. Erk, Z. Bao, F. Würthner, *J. Am. Chem. Soc.* **2009**, *131*, 6215; i) S. Nakazono, Y. Imazaki, H. Yoo, J. Yang, T. Sasamori, N. Tokitoh, T. Cédric, H. Kageyama, D. Kim, H. Shinokubo, A. Osuka, *Chem. Eur. J.* **2009**, *15*, 7530; j) S. Nakazono, S. Easwaramoorthi, D. Kim, H. Shinokubo, A. Osuka, *Org. Lett.* **2009**, *11*, 5426; k) R. K. Dubey, A. Efimov, H. Lemmetyinen, *Chem. Mater.* **2011**, *23*, 778.

[5] See for example: a) P. Osswald, F. Würthner, *J. Am. Chem. Soc.* **2007**, *129*, 14319; b) Y. Shi, H. Qian, Y. Li, W. Yue, Z. Wang, *Org. Lett.* **2008**, *10*, 2337.

[6] T. Riehm, G. De Paoli, A. E. Konradsson, L. De Cola, H. Wadepohl, L. H. Gade, *Chem. Eur. J.* **2007**, *13*, 7317.

[7] a) M. Matena, T. Riehm, M. Stöhr, T. A. Jung, L. H. Gade, *Angew. Chem.* **2008**, *120*, 2448; *Angew. Chem. Int. Ed.* **2008**, *47*, 2414; b) M. Matena, M. Stöhr, T. Riehm, J. Björk, S. Martens, M. S. Dyer, M. Persson, J. Lobo-Checa, K. Müller, M. Enache, H. Wadepohl, J. Zegenhagen, T. A. Jung, L. H. Gade, *Chem. Eur. J.* **2010**, *16*, 2079; c) J. Björk, M. Matena, M. S. Dyer, M. Enache, J. Lobo-Checa, L. H. Gade, T. A. Jung, M. Stöhr, M. Persson, *Phys. Chem. Chem. Phys.* **2010**, *12*, 8815.

[8] a) K. W. Hellmann, C. H. Galka, I. Rüdenauer, L. H. Gade, I. J. Scowen, M. McPartlin, *Angew. Chem.* **1998**, *110*, 2053; *Angew. Chem. Int. Ed.* **1998**, *37*, 1948; b) L. H. Gade, C. H. Galka, K. W. Hellmann, R. M. Williams, L. De Cola, I. J. Scowen, M. McPartlin, *Chem. Eur. J.* **2002**, *8*, 3732; c) L. H. Gade, C. H. Galka, R. M. Williams, L. De Cola, M. McPartlin, L. Chi, B. Dong, *Angew. Chem.* **2003**, *115*, 2781; *Angew. Chem. Int. Ed.* **2003**, *42*, 2677.

[9] S. C. Martens, T. Riehm, S. Geib, H. Wadepohl, L. H. Gade, *J. Org. Chem.* **2011**, *76*, 609.

[10] a) S. C. Martens, U. Zschieschang, H. Wadepohl, H. Klauk, L. H. Gade, *Chem. Eur. J.* **2012**, *18*, 3498; b) S. Geib, U. Zschieschang, M. Gsänger, M. Stolte, F. Würthner, H. Wadepohl, H. Klauk, L. H. Gade, *Adv. Funct. Mater.* **2013**, *23*, 3866.

[11] A. F. Littke, G. C. Fu, *Angew. Chem.* **1998**, *110*, 3586; *Angew. Chem. Int. Ed.* **1998**, *37*, 3387.

[12] a) N. Miyaura, A. Suzuki, *Chem. Rev.* **1995**, *95*, 2457; b) D. Alberico, M. E. Scott, M. Lautens, *Chem. Rev.* **2007**, *107*, 174.

[13] O. V. Gusev, T. A. Peganova, A. M. Kalsin, N. V. Vologdin, P. V. Petrovskii, K. A. Lyssenko, A. V. Tsvetkov, I. P. Beletskaya, *Organometallics* **2006**, *25*, 2750.

[14] J. R. Lakowicz, *Principles of Fluorescence Spectroscopy*, Third Edition, Springer, New York, **2006**.

[15] a) L. Feiler, H. Langhals, K. Polborn, *Liebigs Ann.* **1995**, 1229; b) H. Langhals, *Helv. Chim. Acta* **2005**, *88*, 1309; c) M. Sadrai, G. R. Bird, *Opt. Commun.* **1984**, *51*, 62; d) H.-G. Löhmannsröben, H. Langhals, *Appl. Phys. B* **1989**, *48*, 449; e) W. E. Ford, P. V. Kamat, *J. Phys. Chem.* **1987**, *91*, 6373; f) U. Rohr, P. Schlichting, A. Böhm, M. Groß, K. Meerholz, C. Bräuchle, K. Müllen, *Angew. Chem.* **1998**, *110*, 1463; *Angew. Chem. Int. Ed.* **1998**, *37*, 1434; g) H. Langhals, J. Karolin, L. B. A. Johannson, *J. Chem. Soc. Faraday Trans.* **1998**, *94*, 2919.

[16] N. I. Nijegorodov, W. S. Downey, *J. Phys. Chem.* **1994**, *98*, 5639.

[17] I. Seguy, P. Jolinat, P. Destruel, R. Mamy, H. Allouchi, C. Courseille, M. Cotrait, H. Bock, *ChemPhysChem* **2001**, *2*, 448.

[18] A. Pron, R. R. Reghu, R. Rybakiewicz, H. Cybulski, D. Djurado, J. V. Grazulevicius, M. Zagorska, I. Kulszewicz-Bajer, J.-M. Verilhac, *J. Phys. Chem. C* **2011**, *115*, 15008.

[19] C.-C. Chao, M.-K. Leung, *J. Org. Chem.* **2005**, *70*, 4323.

[20] M. W. Logue, K. Teng, *J. Org. Chem.* **1982**, *47*, 2549.

[21] D. F. Eaton, *Pure Appl. Chem.* **1988**, *60*, 1107.

[22] W. R. Dawson, M. W. Windsor, *J. Phys. Chem.* **1968**, *72*, 3251.

[23] D. Madge, J. H. Brannon, T. L. Cremers, J. Olmsted III, *J. Phys. Chem.* **1979**, *83*, 696.

[24] a) W. J. Hehre, R. Ditchfield, J. A. Pople, *J. Chem. Phys.* **1972**, *56*, 2257; b) J. A. Pople, *J. Chem. Phys.* **1975**, *62*, 2921; c) M. M. Francl, W. J. Pietro, W. J. Hehre, J. S. Binkley, M. S. Gordon, D. J. DeFrees, J. A. Pople, *J. Chem. Phys.* **1982**, *77*, 3654; d) T. Clark, J. Chandrasekhar, G. W. Spitznagel, P. V. R. Schleyer, *J. Comput. Chem.* **1983**, *4*, 294.

[25] M. J. Frisch, G. W. Trucks, H. B. Schlegel, G. E. Scuseria, M. A. Robb, J. R. Cheeseman, J. A. Montgomery, Jr. T. Vreven, K. N. Kudin, J. C. Burant, J. M. Millam, S. S. Iyengar, J. Tomasi, V. Barone, B. Mennucci, M. Cossi, G. Scalmani, N. Rega, G. A. Petersson, H. Nakatsuji, M. Hada, M. Ehara, K. Toyota, R. Fukuda, J. Hasegawa, M. Ishida, T. Nakajima, Y. Honda, O. Kitao, H. Nakai, M. Klene, X. Li, J. E. Knox, H. P. Hratchian, J. B. Cross, V. Bakken, C. Adamo, J. Jaramillo, R. Gomperts, R. E. Stratmann, O. Yazyev, A. J. Austin, R. Cammi, C. Pomelli, J. W. Ochterski, P. Y. Ayala, K. Morokuma, G. A. Voth, P. Salvador, J. J. Dannenberg, V. G. Zakrzewski, S. Dapprich, A. D. Daniels, M. C. Strain, O. Farkas, D. K. Malick, A. D. Rabuck, K. Raghavachari, J. B. Foresman, J. V. Ortiz, Q. Cui, A. G. Baboul, S. Clifford, J. Cioslowski, B. B. Stefanov, G. Liu, A. Liashenko, P. Piskorz, I. Komaromi, R. L. Martin, D. J. Fox, T. Keith, M. A. Al-Laham, C. Y. Peng, A. Nanayakkara, M. Challacombe, P. M. W. Gill, B. Johnson, W. Chen, M. W. Wong, C. Gonzalez, J. A. Pople, Gaussian 03, Revision D.02; Gaussian, Inc.: Wallingford,CT, **2004**.

[26] CrysAlisPro, Agilent Technologies UK Ltd., Oxford **2013**.

[27] a) L. Palatinus, SUPERFLIP, EPF Lausanne, Switzerland, **2007**; b) L. Palatinus, G. Chapuis, *J. Appl. Crystallogr.* **2007**, *40*, 786.

[28] a) G. M. Sheldrick, SHELXL-2013, University of Göttingen, **2013**; b) G. M. Sheldrick, *Acta Crystallogr. Sect. A* **2008**, *64*, 112.

Received: May 17, 2013
Published online: September 11, 2013

